Scientific Reports

https://doi.org/10.1038/s41598-026-36108-x

Article in Press

Adaptive anti-synchronization of transcendental alternated system of Julia sets

Received: 31 October 2025

Accepted: 9 January 2026

Published online: 10 February 2026

Cite this article as: Ravikumar V. & Konar P. Adaptive anti-synchronization of transcendental alternated system of Julia sets. *Sci Rep* (2026). https://doi.org/10.1038/s41598-026-36108-x

Varthini Ravikumar & Pulak Konar

Adaptive anti-synchronization of transcendental alternated system of Julia sets

Varthini **Ravikumar**[a] and Pulak **Konar**[a*]

[a]Department of Mathematics, School of Advanced Sciences

VIT University - Chennai Campus, Vandalur

Kelambakkam Road, Tamil Nadu, 600127, India.

varthini2001@gmail.com, pulakkonar@vit.ac.in, pulakkonar@gmail.com

Abstract

This paper presents an adaptive control strategy for achieving anti-synchronization in transcendental alternated(odd and even functions) Julia sets. The system employs cosine-based transcendental mappings that works alternatively through iteration, generating complex Julia dynamics. Adaptive controllers are developed for both known and unknown set of parameters, with update laws incurred to estimate unknown coefficients of transcendental operators for the iterative schemes. Stability analysis of this artiscle guarantees the convergence of the anti-synchronization error, while numerical results demonstrate rapid convergence and accurate parameter estimation of the control system. The article depicts the computational behavior of the system through the Average Number of Iterations (ANI) and time analysis, providing deeper insight into the convergence dynamics and efficiency of the iterative process. The proposed method enhances the stability and performance of transcendental alternated systems.

*corresponding author: Pulak Konar (pulakkonar@vit.ac.in)

AMS Code: $37F10, 93C40$

Keywords: Iteration; Julia Set; Anti-synchronization; Transcedental alternated system; Control system.

1 Introduction

Fractal theory plays a pivotal role in the analysis of complex nonlinear systems, offering insight into self-similar structures and chaotic dynamics observed in nature and technology. Among various fractals, Julia sets have attracted extensive research attention for their intricate boundaries and sensitivity to initial conditions [1]. The origins of fractal theory can be traced to the early twentieth century, when French mathematicians Gaston Maurice Julia and Pierre Fatou began studying the iterative behavior of complex functions. They examined the nonlinear mapping $f(z) = z^2 + c$, where z and c are complex numbers, in order to understand how successive iterations evolve in the complex plane. Julia (1918) explored the iterative behavior of the function, while Fatou (1919) classified its dynamics by introducing the Fatou set, where nearby points evolve similarly through Julia set, where small perturbations cause divergency and resulting as smooth mapping in the Fatou set but chaotic on the Julia set [2, 3].

On the other hand, iterative systems creates a large amount of literature canvasing the geometric of real banach spaces and provide as control over the convergences(weak, strong) throughout the process [4]. Though the efficiency and computational behaviour of the said system is a bit different, it is still contextual due to iterative process.

The concept of synchronization in nonlinear dynamics, introduced by Pecora and Carroll [5], showed that chaotic systems can evolve coherently through suitable coupling. Later studies extended this idea to several forms, including anti-synchronization, where the system state is stable. This mechanism has drawn attention for its potential in masking signals and enhancing the security of communication systems [6]. In recent years, a number of studies have examined synchronization and control strategies for fractal systems, especially Julia sets. Wang and Liu [7, 8] explored the control and synchronization of alternated Julia systems, while Wang and Zhang [9] developed an adaptive anti-synchronization technique for Julia sets in generalized alternated systems. Their work, based on polynomial iteration mappings, successfully demonstrated synchronization between two distinct fractal systems using adaptive control laws. Futhermore, Wang, Liu, and Li [10] extended the adaptive synchronization framework to Julia sets generated by the Mittag-Leffler function, demonstrating that transcendental-type Julia systems can also achieve robust synchronization through adaptive control. Their work highlights the potential of non-polynomial mappings in revealing novel dynamical structures within fractal synchronization. Similarly, several related studies have contributed to the understanding of synchronization in fractal and nonlinear systems, including feedback control of Mandelbrot sets [11], synchronization of Julia sets in the forced Brusselator model [12], and fractal control in predator–prey systems [13]. Moreover, studies on fractional-order systems [14], Boolean networks [15], and coupled Mandelbrot dynamics [16] further emphasize the universality of synchronization mechanisms across complex systems.

However, the majority of existing research remains focused on polynomial alternated systems, the study of transcendental alternated systems those governed by the trigonometric or exponential functions has been comparatively limited, despite their ability to generate far more diverse and intricate fractal structures. Transcendental functions, particularly those defined by cosine and sine mappings, exhibit stronger nonlinear characteristics and produce more intricate dynamical behaviors compared to polynomial functions. These distinctive features motivate the extension of adaptive synchronization methods to transcendental systems, aiming to explore new dynamical phenomena and broaden their applications [17, 18].

In addition to synchronization analysis, the present work integrates Average Number of Iterations (ANI) and time calculation techniques to investigate the computational characteristics of the proposed transcendental alternated Julia system. The ANI framework enables detailed visualization of fractal evolution during the iterative process, providing deeper insight into convergence trends and dynamic stability. Simultaneously, time calculation is employed to measure the computational duration of each pixel during fractal generation, thereby quantifying how adaptive control laws and system parameters affect iteration speed and convergence behavior. This time-based evaluation offers a valuable link between theoretical dynamics and computational performance, supporting the validation of the proposed model [19, 20, 21]. Recent studies on adaptive estimation have explored how uncertainty is handled in discrete-time systems. Although developed in different contexts, these ideas provide useful background for the adaptive framework considered in this work [22, 23, 24]

The structure of the paper is outlined as follows: Section 2 introduces the mathematical preliminaries. Section 3 presents the adaptive anti-synchronization control laws for both known and unknown parameter cases. Section 4 provides numerical simulations validating the theoretical results. Section 5 discusses the implementation of the ANI and time calculation schemes, and Section 6 concludes the paper.

2 Preliminaries

Definition 1. *Let $G_c : \mathbb{C} \to \mathbb{C}$ be a complex-valued function that depends on a complex parameter $c \in \mathbb{C}$. The filled Julia set associated with G_c, denoted by K_{G_c}, is defined as*

$$K_{G_c} = \left\{ z \in \mathbb{C} : \left\{ G_c^{(q)}(z) \right\}_{q=0}^{\infty} \text{ is bounded} \right\},$$

where $G_c^{(q)}$ represents the q-th iterate of G_c. The Julia set of G_c is given by the boundary of the filled Julia set:

$$J_{G_c} = \partial K_{G_c}.$$

In addition, the Julia set J_f exhibits the following fundamental properties:

1. *The Julia set J_f is always bounded and nonempty.*

2. *The set J_f satisfies the property of complete invariance under the function f, satisfying $J_f = f(J_f) = f^{-1}(J_f)$.*

3. *For any positive integer p, the Julia set remains invariant under iteration, that is, $J_f = J_{f^p}$.*

4. *If f possesses an attracting fixed point ξ, then the Julia set J_f corresponds to the boundary of its attractive domain $A(\xi)$, expressed as $J_f = \partial A(\xi)$.*

Definition 2. *For any initial conditions $z_0, w_0 \in \mathbb{C}$ corresponding to driving and response system, an adaptive control input u_m can be designed such that*

$$\lim_{m\to\infty} \|e_m\| = \lim_{m\to\infty} \|z_m + w_m\| = 0.$$

This condition implies that the trajectories of the two systems exhibit anti-synchronization, meaning the state variables z_m and w_m evolve in a way that their combined error asymptotically vanishes. Consequently, the corresponding Julia sets of the driving and response systems demonstrate anti-synchronous behavior.

3 Adaptive Anti-synchronization of alternated transcendental system

Considering the transcendental alternated system, the iterative map G_c alternates its form depending on the iteration index m, and is defined as:

$$G_c(z_m) = \begin{cases} \alpha \cos^p(z_m) + \beta_1, & \text{if } m \text{ is even,} \\ \alpha \cos^p(z_m) + \beta_2, & \text{if } m \text{ is odd,} \end{cases}$$

where $\alpha \in \mathbb{R}$, $p \in \mathbb{N}$, $\cos^p(z_m) \neq 0$ for all m and $\beta_1, \beta_2 \in \mathbb{C}$ with $\beta_1 \neq \beta_2$. Accordingly, the filled Julia set K_{G_c} is defined as the set of initial points $z_0 \in \mathbb{C}$ for which the trajectory generated by the alternated iteration of G_c remains bounded.

3.1 Adaptive antisynchronization of julia sets through transcendental systems

In the analysis of anti-synchronization of Julia sets within transcendental alternated systems, we introduce the driving system as:

$$z_{m+1} = \begin{cases} \alpha \cos^p(z_m) + \beta_1, & m \text{ is even,} \\ \alpha \cos^p(z_m) + \beta_2, & m \text{ is odd.} \end{cases} \tag{3.1}$$

The response system is defined as:

$$w_{m+1} = \begin{cases} \gamma \cos^q(\omega_m) + \beta_3 + u_m, & m \text{ is even} \\ \gamma \cos^q(\omega_m) + \beta_4 + u_m, & m \text{ is odd} \end{cases} \tag{3.2}$$

in which $\alpha, \gamma \in \mathbb{R}$, $p \in \mathbb{N}$, $\beta_i \in \mathbb{C}$ $(i = 1, 2, 3, 4)$ with $\beta_1 \neq \beta_2$, $\beta_3 \neq \beta_4$, $\cos^p(z_m) \neq 0$ and $\cos^q(w_m) \neq 0$. for all m and u_m stands for the adaptive controller to be developed. The anti-synchronization error between the driving and response systems is defined as

$$e_{m+1} = z_{m+1} + w_{m+1}, \tag{3.3}$$

where the error can be expressed in terms of its real and imaginary components as $e_{m+1} = e^r_{m+1} + ie^j_{m+1}$. Here, e^r_{m+1} and e^j_{m+1} denote the real and imaginary parts of the error, respectively.

Case 1: Known Parameters α and γ

When both α and γ are assumed to be known for the chosen values of p and q, the adaptive controller is designed as

$$u_m = \begin{cases} -(\alpha \cos^p(z_m) + \beta_1) - (\gamma \cos^q(w_m) + \beta_3) - ke_m, & m \text{ is even}, \\ -(\alpha \cos^p(z_m) + \beta_2) - (\gamma \cos^q(w_m) + \beta_4) - ke_m, & m \text{ is odd}, \end{cases} \tag{3.4}$$

Whenever $|k| < 1$, the response system (3.2) and the driving system (3.1) attain anti-synchronization of their Julia sets, regardless of the choice of initial conditions z_0 and w_0.

Proof. The error is given by

$$e_{m+1} = z_{m+1} + w_{m+1}.$$

By substituting the dynamics of the driving system, the response system, and the controller into this expression, we obtain

$$e_{m+1} = \begin{cases} \alpha \cos^p(z_m) + \beta_1 + \gamma \cos^q(w_m) + \beta_3 - (\alpha \cos^p(z_m) + \beta_1 + \gamma \cos^q(w_m) + \beta_3) - ke_m, & m \text{ is even}, \\ \alpha \cos^p(z_m) + \beta_2 + \gamma \cos^q(w_m) + \beta_4 - (\alpha \cos^p(z_m) + \beta_2 + \gamma \cos^q(w_m) + \beta_4) - ke_m, & m \text{ is odd}. \end{cases}$$

$= ke_m.$

Given $|k| < 1$,so the error sequence e_m converges to zero as $m \to \infty$. Considering Definition 2, this guarantees that the trajectories of Systems (3.1) and (3.2) reach anti-synchronization. Therefore, the Julia sets of the two systems are anti-synchronized, which completes the proof. □

Case 2: Unknown Parameter α and Known Parameter γ In this case, we assume that the parameter α is unknown, while γ is known for the chosen values of p and q. To handle the uncertainty in α, we design an adaptive controller with an estimated value $\hat{\alpha}_m$ of α. The controller is given by

$$u_m = \begin{cases} -(\hat{\alpha}_m \cos^p(z_m) + \beta_1) - (\gamma \cos^q(w_m) + \beta_3) - ke_m, & m \text{ is even,} \\ -(\hat{\alpha}_m \cos^p(z_m) + \beta_2) - (\gamma \cos^q(w_m) + \beta_4) - ke_m, & m \text{ is odd.} \end{cases} \tag{3.5}$$

To update the parameter estimate $\hat{\alpha}_m$, we introduce the following adaptive law:

$$\hat{\alpha}_{m+1} = \hat{\alpha}_m + d\, \frac{e_{m+1} \cos^p(z_m) - e_m \cos^p(z_{m+1})}{\cos^p(z_m) \cos^p(z_{m+1})}, \tag{3.6}$$

where $d, k \in \mathbb{R}$ and $|d + k| < 1$.For any initial conditions z_0, w_0 and $\hat{\alpha}_0$, the anti-synchronization between the Julia sets of the response system (3.2) and the driving system (3.1) is achieved.

Proof.

$$e_m = z_{m+1} + w_{m+1}$$

$$= \begin{cases} \alpha \cos^p z_m + \beta_1 + \gamma \cos^q w_m + \beta_3 - (\hat{\alpha}_m \cos^p z_m + \beta_1) - (\gamma \cos^q w_m + \beta_3) - ke_m, & n \text{ is even,} \\ \alpha \cos^p z_m + \beta_2 + \gamma \cos^q w_m + \beta_4 - (\hat{\alpha}_m \cos^p z_m + \beta_2) - (\gamma \cos^q w_m + \beta_4) - ke_m, & n \text{ is odd} \end{cases}$$

$$= (\alpha - \hat{\alpha}_m)\cos^p z_m - ke_m$$

where $\tilde{\alpha}_m = \alpha - \hat{\alpha}_m$. From Equation (3.6), we obtain

$$\hat{\alpha}_{m+1} - \hat{\alpha}_m = d\,\frac{e_{m+1}\cos^p(z_m) - e_m\cos^p(z_{m+1})}{\cos^p(z_m)\cos^p(z_{m+1})}.$$

This can be rewritten as

$$\hat{\alpha}_{m+1} - \alpha - (\hat{\alpha}_m - \alpha) = \frac{de_{m+1}}{\cos^p(z_{m+1})} - \frac{de_m}{\cos^p(z_m)}.$$

Since the parameter update at step n only depends on z_m and e_m, it follows that

$$\hat{\alpha}_m - \alpha = \frac{de_m}{\cos^p(z_m)}.$$

Therefore, the parameter estimation error can be expressed as

$$\tilde{\alpha}_m = \alpha - \hat{\alpha}_m = -\frac{de_m}{\cos^p(z_m)} \tag{3.7}$$

Substituting (3.7) into the error dynamics, we obtain

$$e_{m+1} = (\alpha - \hat{\alpha}_m)\cos^p(z_m) - ke_m = -\frac{de_m}{\cos^p(z_m)}\cos^p(z_m) - ke_m = -(d+k)e_m.$$

If the control parameters d and k satisfy the condition $|d+k| < 1$, then the error sequence $\{e_m\}$ converges to zero as $m \to \infty$. Hence, the trajectories of the driving system (3.1) and the response system (3.2) attain anti-synchronization, and the adaptive law ensures that $\hat{\alpha}_m$ successfully estimates the true parameter α. This concludes the proof. □

Case 3: Unknown Parameters α and γ

Now suppose that both system parameters α and γ are unknown while p and q remain fixed. Let $d, t, k \in \mathbb{R}$ be chosen such that the condition $|d + t + k| < 1$ holds. In this setting, the adaptive controller is constructed as

$$u_m = \begin{cases} -(\hat{\alpha}_m \cos^p(z_m) + \beta_1) - (\hat{\gamma}_m \cos^q(w_m) + \beta_3) - ke_m, & m \text{ is even,} \\ \\ -(\hat{\alpha}_m \cos^p(z_m) + \beta_2) - (\hat{\gamma}_m \cos^q(w_m) + \beta_4) - ke_m, & m \text{ is odd.} \end{cases} \tag{3.8}$$

and the update laws of $\hat{\alpha}_m$ and $\hat{\gamma}_m$ are

$$\begin{cases} \hat{\alpha}_{m+1} = \hat{\alpha}_m + \dfrac{d\,(e_{m+1} \cos^p(z_m) - e_m \cos^p(z_{m+1}))}{\cos^p(z_m)\cos^p(z_{m+1})} \\ \hat{\gamma}_{m+1} = \hat{\gamma}_m + \dfrac{t\,(e_{m+1} \cos^q(w_m) - e_m \cos^q(w_{m+1}))}{\cos^q(w_m)\cos^q(w_{m+1})} \end{cases} \tag{3.9}$$

For any chosen initial conditions (z_0, w_0) and $(\hat{\alpha}_0, \hat{\gamma}_0)$, the driving system and the response system of the Julia sets, that are (3.1) and (3.2) respectively achieve anti-synchronization, where $\hat{\alpha}_m$ and $\hat{\gamma}_m$ are the estimates of the unknown parameters α and γ.

Proof.

$$e_m = z_{m+1} + w_{m+1}$$

$$= \begin{cases} \alpha \cos^p z_m + \beta_1 + \gamma \cos^q w_m + \beta_3 - (\hat{\alpha}_m \cos^p z_m + \beta_1) - (\hat{\gamma} \cos^q w_m + \beta_3) - ke_m, & n \text{ is even,} \\ \\ \alpha \cos^p z_m + \beta_2 + \gamma \cos^q w_m + \beta_4 - (\hat{\alpha}_m \cos^p z_m + \beta_2) - (\hat{\gamma} \cos^q w_m + \beta_4) - ke_m, & n \text{ is odd} \end{cases}$$

$$= (\alpha - \hat{\alpha}_m) \cos^p z_m + (\gamma - \hat{\gamma}_m) \cos^q w_m - ke_m$$

From the update law (3.9), we have

$$(\hat{\alpha}_{m+1} - \alpha) - (\hat{\alpha}_m - \alpha) = \frac{de_{m+1}}{\cos^p z_{m+1}} - \frac{de_m}{\cos^p z_m}, \tag{3.10}$$

and

$$(\hat{\gamma}_{m+1} - \gamma) - (\hat{\gamma}_m - \gamma) = \frac{te_{m+1}}{\cos^q w_{m+1}} - \frac{te_m}{\cos^q w_m}. \tag{3.11}$$

As in Case 2, Equation(3.10) shows that the parameter α_m at the n-th step is influenced only by z_m and the error e_m. Likewise, Equation (3.11) demonstrates that the parameter γ_m at step n is determined entirely by w_m which gives,

$$\tilde{\alpha} = \hat{\alpha}_m - \alpha = \frac{de_m}{\cos^p z_m}, \qquad \tilde{\alpha} = \hat{\gamma}_m - \gamma = \frac{te_m}{\cos^q w_m}. \tag{3.12}$$

Using Equation (3.12) in Equation (3.10) & (3.11) gives

$$e_m = (\alpha - \hat{\alpha}_m)\cos^p z_m + (\gamma - \hat{\gamma}_m)\cos^q w_m - ke_m = -(d + t + k)e_m.$$

Provided that the parameters d, t, and k satisfy the condition $|d+t+k| < 1$, it follows that the error term $|e_m|$ converges to zero as $m \to \infty$. In accordance with Definition 2, this convergence implies that the trajectories of both the systems (3.1) and (3.2) exhibit anti-synchronization. Consequently, the adaptive update laws enable accurate identification of the unknown parameters $\hat{\alpha}_m$ and $\hat{\gamma}_m$. This completes the proof. □

4 Numerical example

This section presents numerical simulations of the driving and response systems defined in (3.1) & (3.2) to demonstrate the effectiveness of the proposed adaptive anti-synchronization scheme for transcendental alternated Julia sets.

By taking the following parameter values: $\alpha = 1.5,\ p = 2,\ \beta_1 = 0.1 - 0.2i,\ \beta_2 = 0.5 + 0.2i,\ \gamma = 1.1,\ q = 2,\ \beta_3 = 0.5 + 0.2i,\ \beta_4 = 0.5 - 0.12i,\ k = 0.1,\ e = 0.8 + 2.6i$, Figure 1a illustrates the Julia set of the driving system (3.1), while Figure 1b shows the Julia set of the response system (3.2) without control. In Figure 1c, both Julia sets are superimposed, where the blue curve corresponds to the driving system and the red curve represents the response system. It can be observed that the two Julia sets overlap closely, confirming that the response system achieves anti-synchronization with the driving system. This overlap demonstrates the effectiveness of the proposed adaptive control scheme and indicates that the transcendental alternated system for secure communication and encryption applications.

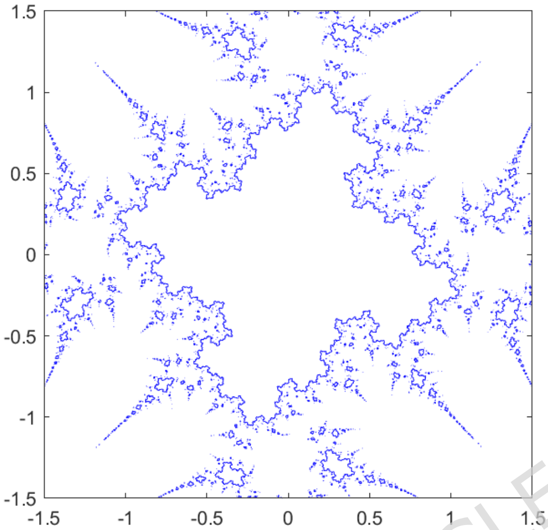

(a) The original Julia set of System (3.1)

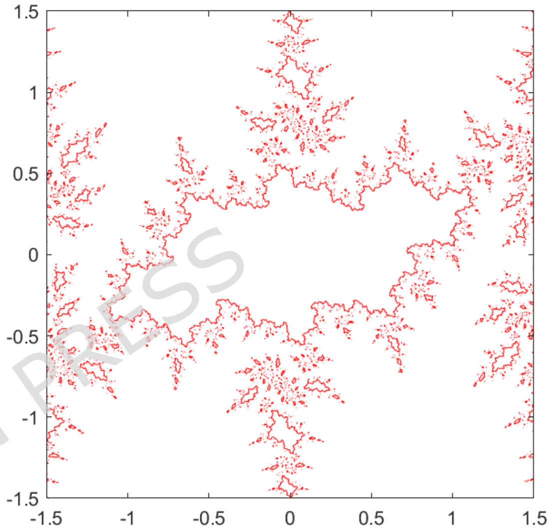

(b) The original Julia set of System (3.2)

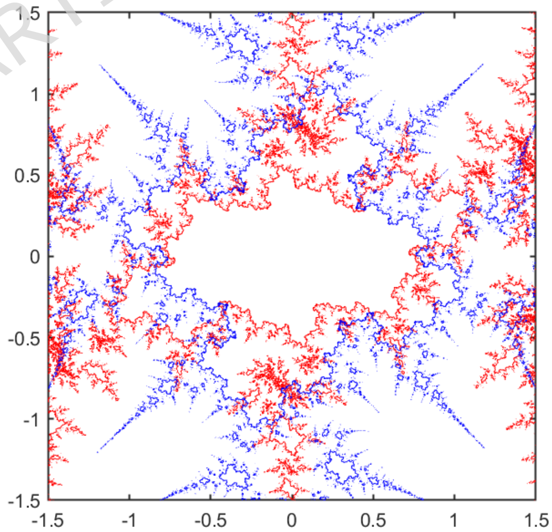

(c) The anti-synchronization of Julia sets between Systems (3.1) and (3.2)

Figure 1: The Julia sets of the systems

Case 1: To examine the effect of the parameter k on the convergence rate of the anti-synchronization error e_m, simulations were conducted using the initial condition $e_0 = 3.5 + 0.1i$. The results, presented in Figure 2, demonstrate that the convergence speed of e_m is inversely related to the magnitude of k. Specifically, smaller values of k yield faster error decay, confirming the sensitivity of the system's synchronization dynamics to this parameter.

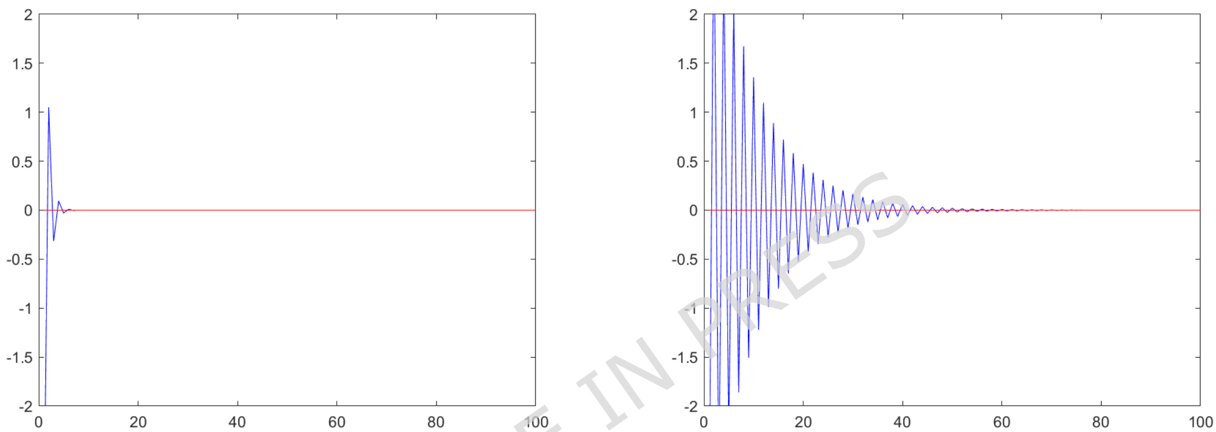

Error when $k = 0.3$ Error when $k = 0.9$

Figure 2: The anti-synchronization error by varying the parameter k

Case 2: To investigate the influence of the parameter $|d+k|$ on the convergence rate of the anti-synchronization error e_m, numerical simulations were performed. The results, depicted in Figure 3, reveal that the convergence speed of e_m is inversely proportional to the magnitude of $|d+k|$. In particular, smaller values of $|d+k|$ lead to more rapid error attenuation, emphasizing the parameter's critical role in shaping the system's synchronization behavior.

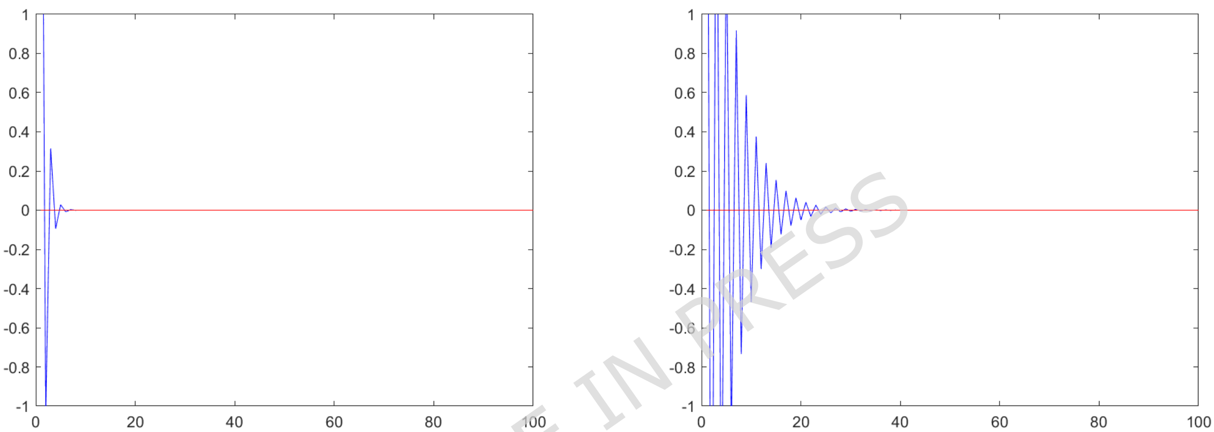

Error when $|d+k| = 0.3$ Error when $|d+k| = 0.8$

Figure 3: The anti-synchronization error by varying the parameter $|d+k|$

Case 3: To evaluate the effect of the parameter $|d+t+k|$ on the convergence rate of the anti-synchronization error e_m, numerical results are presented in Figure 4. The figure clearly demonstrates that the speed at which e_m approaches zero is governed by the magnitude of $|d+t+k|$. In particular, smaller values of $|d+t+k|$ lead to faster error convergence, highlighting its significance in enhancing the system's synchronization dynamics.

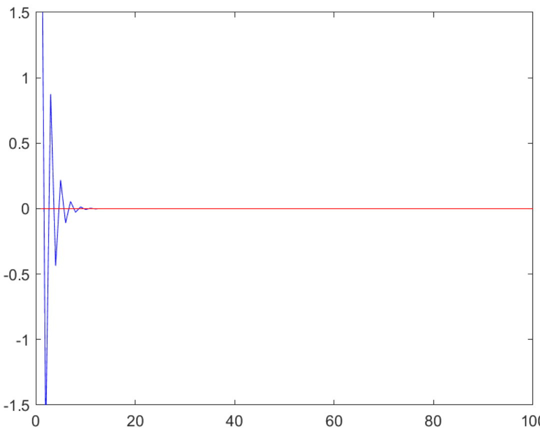

Error when $|d+t+k| = 0.5$

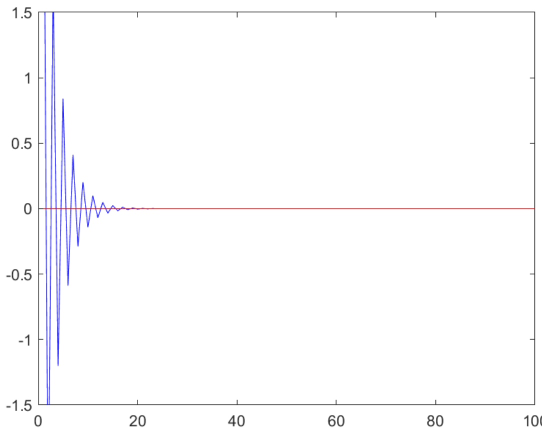

Error when $|d+t+k| = 0.7$

Figure 4: The anti-synchronization error by varying the parameter $|d+t+k|$

In Systems (3.1) and (3.2), the parameters α and γ are initially unknown. To initiate the estimation process, the systems were assigned initial conditions $z_0 = 0.52 - 0.01i$ and $w_0 = 0.33 + 1.25i$, respectively. The initial guesses for the unknown parameters were set as $\alpha_0 = 2$ and $\gamma_0 = 1$, with the anti-synchronous error initialized at $e_0 = 3$. Figure 5 presents the evolution of the parameter estimates, illustrating the identification of $\hat{\alpha}$ and $\hat{\gamma}$ over time.

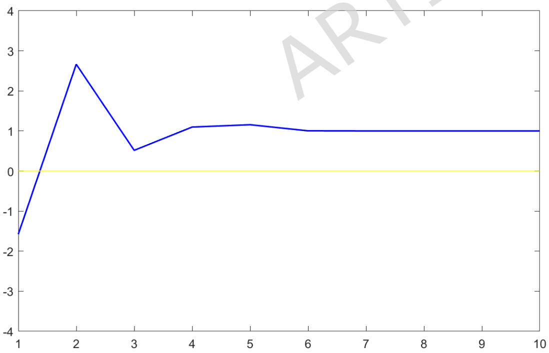

The estimation of parameter α

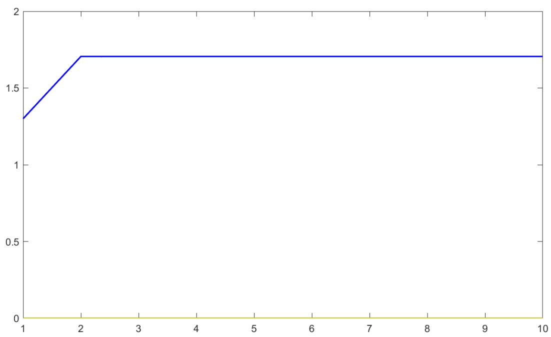

The estimation of parameter γ

Figure 5: The estimation of parameter under adaptive controller

5 ANI and Time calculations for Julia Set

The Average Number of Iterations (ANI) and execution time are essential parameters for evaluating the performance of Julia set. ANI denotes the average iterations required for complex points to either escape to infinity or remain bounded, thereby indicating the convergence efficiency and stability of the iterative scheme. In the ANI and time-distribution plots, the x axis and y axis represent the real and imaginary parts of the initial complex point z_0, respectively, while the color scale, displayed using a turbo colormap [Figure 6], indicates the average number of iterations or the computation time generated by the transcendental cosine mapping.

Figure 6: Color scheme used in simulations

The Average Number of Iterations (ANI) was evaluated to study the convergence performance of the proposed adaptive anti-synchronization system. Simulations were performed in MATLAB using a 100×100 complex grid, with an escape radius of 20 and a maximum of 100 iterations. The alternating complex parameters were set as $\beta_1 = 0.1 - 0.2i, \quad \beta_2 = 0.5 + 0.2i$, with the exponent fixed at $p = 2$. To study the effect of parameter variation on convergence behavior, simulations were performed for $\alpha = 0.92$ and $\alpha = 1.45$, keeping the remaining parameters unchanged (see Figure 7).

The results show that for $\alpha = 0.92$ the average ANI is 4.7193 (min = 0.6270, max = 9.3780), while for $\alpha = 1.45$ the average ANI reduces to 2.0334 (min = 0.1780, max = 5.7880) demonstrating enhanced convergence with the higher parameter value. Overall, these findings confirm that the proposed system achieves stable and efficient convergence in generating transcendental alternated Julia sets.

The execution time was also analyzed to evaluate the computational efficiency of the

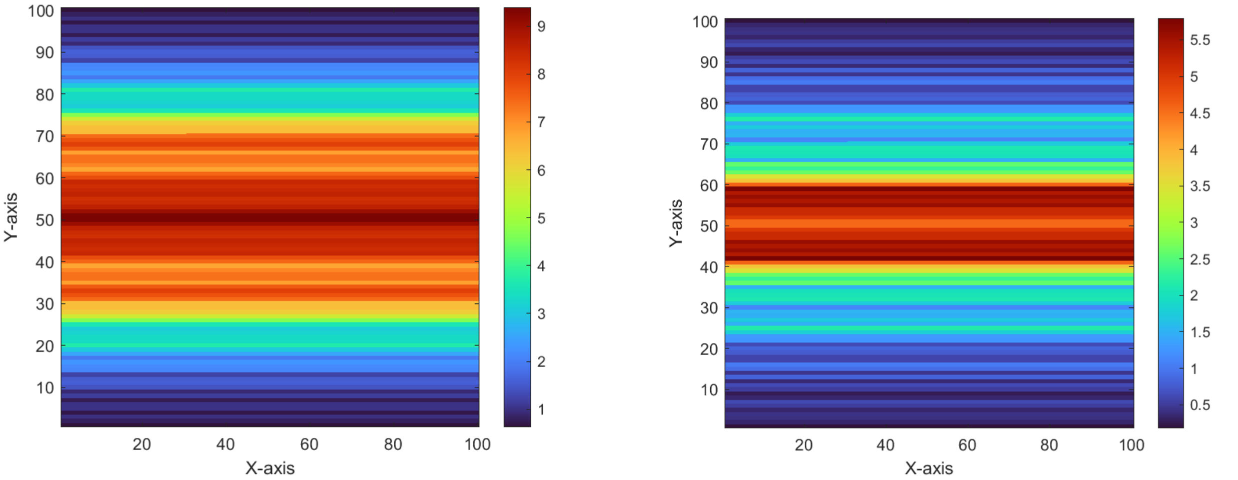

$\alpha = 0.92$ $\alpha = 1.45$

Figure 7: ANI values by varying α

proposed system under different parameter conditions. The same simulation setup was used as in the ANI analysis, with a 100×100 complex grid, an escape radius of 20, and a maximum of 100 iterations. The alternating parameters $\beta_1 = 0.1 - 0.2i$, $\beta_2 = 0.5 + 0.2i$, and $p = 2$ were fixed, while varying the parameter as $\alpha = 0.92$ and $\alpha = 1.45$.

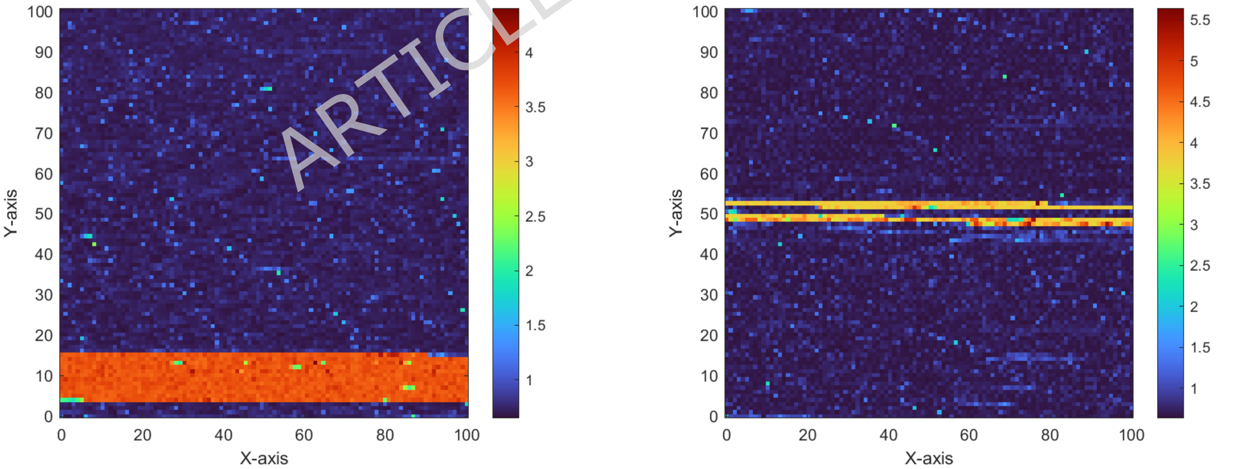

$\alpha = 0.92$ $\alpha = 1.45$

Figure 8: Time calculation by varying the parameter α

The obtained average execution time was approximately 0.0162m for $\alpha = 0.92$ and 0.0104m for $\alpha = 1.45$ (see Figure 8). The corresponding time distributions are illustrated in the above figures. These results clearly show that a higher parameter value leads to reduced computation time, confirming that the proposed algorithm achieves faster and more efficient execution in generating transcendental alternated Julia sets.

6 Conclusion

In this paper, we proposed an adaptive control system to achieve anti-synchronization in transcendental alternated Julia systems using cosine-based transcendental mappings. Adaptive laws were formulated to handle both known and unknown parameters, ensuring stability and accurate estimation. Theoretical analysis and numerical results confirmed rapid convergence and robust performance of the proposed approach. Additionally, Average Number of Iterations (ANI) and time calculation were performed to assess computational efficiency, revealing faster convergence and reduced execution time for higher parameter values. Overall, the proposed transcendental alternated system enhances both stability and computational efficiency. Some engineering application with strong potential for practical applications in the field of image encryption can be seen in [25, 26, 27]. The scope of the article here to discuss the theoretical impact of the adaptive laws but the work of image encryption can be collaboratively taken up in future.

Conflict of interest

The authors declare that they have no known competing financial interests or personal relationships that could have appeared to influence the work reported in this paper.

Data availability statement

The datasets used and/or analysed during the current study available from the corresponding author on reasonable request.

Authorship contribution statement

All authors made equal and substantial contributions to the conception, development, and completion of this work. V. R performed the methodology and computations. P.K conceptualized and supervised the findings of this work.

Funding

This research does not received any external funding.

References

[1] K. Falconer, Fractal geometry: mathematical foundations and applications, John Wiley & Sons, 2013.

[2] G. Julia, Mémoire sur l'itération des fonctions rationnelles, Journal de mathématiques pures et appliquées 1 (1918) 47–245.

[3] S. M. de France, Bulletin de la Société mathématique de France, Vol. 1, La Société, 1875.

[4] P. Sujitha, P. Konar, N. Nathiya, A new iterative scheme for optimal convergence in equilibrium problems, Mathematical methods in the applied sciences (2025).

[5] L. M. Pecora, T. L. Carroll, Synchronization in chaotic systems, Physical review letters 64 (8) (1990) 821.

[6] T.-L. Liao, S.-H. Tsai, Adaptive synchronization of chaotic systems and its application to secure communications, Chaos, Solitons & Fractals 11 (9) (2000) 1387–1396.

[7] P. Wang, S. Liu, The gradient control of spatial-alternated julia sets, Nonlinear Dynamics 80 (3) (2015) 1291–1302.

[8] P. Wang, S. Liu, Control of julia sets in generalized alternated system, Asian Journal of Control 18 (6) (2016) 2234–2243.

[9] P. Wang, H. Zhang, Adaptive anti-synchronization of julia sets in generalized alternated system, IEEE Access 8 (2020) 175596–175601.

[10] Y. Wang, S. Liu, H. Li, Adaptive synchronization of julia sets generated by mittag-leffler function, Communications in Nonlinear Science and Numerical Simulation 83 (2020) 105115.

[11] Y.-P. Zhang, Feedback control and synchronization of mandelbrot sets, Chinese Physics B 22 (1) (2013) 010502.

[12] W. Sun, Y. Zhang, Control and synchronization of julia sets in the forced brusselator model, International Journal of Bifurcation and Chaos 25 (09) (2015) 1550113.

[13] W. Sun, Y. Zhang, X. Zhang, Fractal analysis and control in the predator–prey model, International Journal of Computer Mathematics 94 (4) (2017) 737–746.

[14] X. Liu, L. Hong, Chaos and adaptive synchronizations in fractional-order systems, International Journal of Bifurcation and Chaos 23 (11) (2013) 1350175.

[15] H. Chen, Y. Liu, J. Lu, Synchronization criteria for two boolean networks based on logical control, International Journal of Bifurcation and Chaos 23 (11) (2013) 1350178.

[16] Y. Zhang, W. Sun, Synchronization and coupling of mandelbrot sets, Nonlinear Dynamics 64 (1) (2011) 59–63.

[17] D. J. Prajapati, S. Rawat, A. Tomar, M. Sajid, R. Dimri, A brief study on julia sets in the dynamics of entire transcendental function using mann iterative scheme, Fractal and Fractional 6 (7) (2022) 397.

[18] K. H. Alam, Y. Rohen, A. Tomar, N. Saleem, M. Aphane, A. Razzaque, An effective iterative process utilizing transcendental sine functions for the generation of julia and mandelbrot sets, Fractal and Fractional 9 (1) (2025) 40.

[19] A. Tassaddiq, M. Tanveer, M. Arshad, R. Alharbi, R. M. Kasmani, Fractal generation and analysis using modified fixed-point iteration, AIMS Mathematics 10 (4) (2025) 9462–9492.

[20] S. Nandi, A. Al-Rawashdeh, P. Konar, Non-linearity of the dynamics of transcendental function using fibonacci–mann iteration and some critical remarks, Alexandria Engineering Journal 117 (2025) 1–12.

[21] V. Ravikumar, P. Konar, Complex dynamics and fractals through viscosity approximation method with s-convexity, The European Physical Journal Special Topics (2025) 1–26.

[22] A. Khan, W. Xie, B. Zhang, L.-W. Liu, A survey of interval observers design methods and implementation for uncertain systems, Journal of the Franklin institute 358 (6) (2021) 3077–3126.

[23] A. Khan, X. Bai, B. Zhang, P. Yan, Interval state estimator design for linear parameter varying (lpv) systems, IEEE Transactions on Circuits and Systems II: Express Briefs 68 (8) (2021) 2865–2869.

[24] A. Khan, W. Xie, L.-W. Liu, Set-membership interval state estimator design using observability matrix for discrete-time switched linear systems, IEEE Sensors Journal 20 (11) (2020) 6121–6129.

[25] F. Masood, J. Ahmad, S. A. Shah, S. S. Jamal, I. Hussain, A novel hybrid secure image encryption based on julia set of fractals and 3d lorenz chaotic map, Entropy 22 (3) (2020) 274.

[26] W. Gao, J. Sun, W. Qiao, X. Zhang, Digital image encryption scheme based on generalized mandelbrot-julia set, Optik 185 (2019) 917–929.

[27] M. Kaur, V. Kumar, A comprehensive review on image encryption techniques., Archives of Computational Methods in Engineering 27 (1) (2020).